Acta Neuropathol (2000) 100:29–35

REGULAR PAPER

Francisco García-Sierra · Jean J. Hauw
Charles Duyckaerts · Claude M. Wischik
José Luna-Muñoz · Raúl Mena

The extent of neurofibrillary pathology in perforant pathway neurons is the key determinant of dementia in the very old

Received: 23 April 1999 / Revised: 27 July 1999, 11 October 1999 / Accepted: 12 October 1999

Abstract Neurofibrillary pathology as found in Alzheimer's disease (AD) is also found in the normal elderly, suggesting that these changes may be part of the aging process. In this study, we assessed the densities and distribution of structures recognized by the monoclonal antibody (mAb) to phosphorylated tau (AT8) in the hippocampal formation and medial temporal isocortex of 19 centenarians. Of these, 4 cases were demented and 15 non-demented. AT8 immunoreactivity correlated with the global deterioration scale (GDS). The density of both intraneuronal neurofibrillary tangles (I-NFTs) and neuritic clusters (NCs) significantly correlated with the GDS in the layer II of the entorhinal cortex ($r = 0.66$, $P = 0.005$ and $r = 0.611$, $P = 0.01$, respectively). Density of I-NFTs in the subiculum ($r = 0.491$; $P = 0.034$) also correlated significantly. No other area was found to be statistically significant. Importantly, no correlation was found when demented and non-demented centenarian cases were analyzed separately, suggesting that the difference marks a fundamental shift between AD and non-demented individuals. This assertion is supported by the significantly higher densities of I-NFTs and NCs in the transentorhinal ($P = 0.043$ and $P = 0.011$, respectively) and layer II of the entorhinal cortex ($P = 0.02$ and $P = 0.007$, respectively), and I-NFTs in the subiculum ($P < 0.001$) and CA1 ($P = 0.011$) in the demented group when compared with the non-demented cases. Granular diffuse deposits, an early stage parameter of the neurofibrillary pathology involving accumulation of non-fibrillar abnormally phosphorylated tau protein did not correlate with the GDS or between the two groups studied. This study, combining morphometric and confocal analyses, not only provides further evidence that, in the brains of patients with AD, the perforant pathway is highly sensitive to tau pathology but also that involvement is distinct from the changes of normal aging, even of the oldest old.

Key words Alzheimer's disease · AT8 · Hyperphosphorylated tau protein · Neurofibrillary tangles · Entorhinal cortex

F. García-Sierra · J. Luna-Muñoz · R. Mena (✉)
Department of Physiology, Biophysics and Neurosciences,
CINVESTAV-IPN, PO Box 14-740,
07000, México, D. F., México
e-mail: rmena@fisio.cinvestav.mx,
Tel.: +525-747-7000 ext 5129; Fax: +525-747-7105

J. J. Hauw · C. Duyckaerts
Laboratoire de Neuropathologie R. Escourolle,
Hôpital de la Salpêtrière, Paris, France

C. M. Wischik
Department of Mental Health,
University of Aberdeen, Aberdeen, UK

Introduction

Alzheimer's disease (AD) is histopathologically characterized by the presence of neuritic plaques (NPs), neurofibrillary tangles (NFTs) and neuropil threads (NTs) distributed along transentorhinal and entorhinal cortices, the hippocampal formation and the isocortex. Similar pathological changes are also found in normal elderly subjects [17, 26, 32, 37], although in lesser amounts than in AD.

The distribution of fibrillar and non-fibrillar pathology in isocortical areas has been considered a major criteria for the accurate diagnosis of AD [16, 27] since it is not severly affected in aging. On the other hand, neurofibrillary changes in the entorhinal cortex and hippocampus are often present in non-demented elderly people. For this reason, the histopathological changes in these areas have not been considered diagnostic for AD [3, 16, 27]. Determining if the range of neuropathological and clinical changes described in the elderly [1, 6, 17, 26, 32, 37] actually represent pre-clinical stages of AD or are alterations merely related to normal aging is a major issue in understanding AD. In this study, we address this issue by studying the histopathology in the hippocampus of a cohort of centenarians with the goal of determining if the changes of AD are distinct from aging.

Abnormally phosphorylated microtubule-associated tau protein is a conspicuous component of the paired helical

filaments (PHFs) which accumulate in degenerating neurons in AD [12, 15, 28]. Phosphorylation of serines 199, 202 and threonine 205 in the PHF-associated tau protein is specifically recognized by the monoclonal antibody (mAb) AT8 [4, 20, 21]. Nevertheless, phosphorylated tau protein is also found by immunoblotting in both AD and control individuals aged over 70 years [39].

Previous analyses of very old normal subjects showed that neurofibrillary changes, while present, were less frequent than in AD cases [25]. In a group of demented centenarians, neurofibrillary changes were distributed in the CA1 of the hippocampus as well as the neocortex, an area preserved at the earliest stages of AD in younger cases [18, 19].

In the present study, using conventional and confocal microscopy we immunocytochemically assessed the densities and distribution of AT8-immunoreactive (IR) structures in the hippocampal formation and superior temporal isocortex of 19 centenarian cases. The quantitative data were correlated with the global deterioration scale (GDS) a clinical parameter of cognitive state. Our findings support a distinct increase in neurofibrillary pathology with onset of dementia.

Material and methods

Cases

Clinical and neuropathological data for the 19 centenarian cases studied have been previously reported [13, 14, 24]. The severity of the mental deterioration was retrospectively staged according to the GDS. The series included 15 cases classified as non-demented (GDS ≤ 3), and 4 demented cases; 1 affected with AD and 3 with mixed dementia (combined vascular and AD changes). Brains were fixed in formalin and embedded in paraffin. Adjacent sections, 7 μm thick, from the superior temporal gyrus, hippocampal formation and entorhinal cortex were obtained and used for immunocytochemistry with mAb AT8.

Immunocytochemistry

Prior to the immunolabeling, deparaffinized sections were incubated in 0.5% hydrogen peroxide-phosphate buffered saline (PBS) to inactivate endogeneous peroxidase. Specimens were then incubated with the primary mAb AT8 (I:500) diluted in PBS containing 0.2% Triton X-100, for 1 h at room temperature. A goat anti-mouse immunoglobulin horseradish peroxidase conjugate (HRP) was used as secondary antibody for 1 h. Bound peroxidase was revealed by the addition of 0.06% diaminobenzidine and 0.01% hydrogen peroxide in PBS (pH 7.4). When the reaction was completed slides were washed by immersion in PBS. For morphometry sections were counterstained with hematoxylin, then dehydrated and mounted in DPX.

Morphometry and statistics

Counts of AT8-IR structures were performed blindly to the clinical diagnosis. The density of NFTs in the hippocampal formation and entorhinal cortex was established by counting three adjacent fields per section randomly chosen in each sub-area. For the superior temporal gyrus, the measurements were made in six fields in the vicinity of the sulcus. Identification and counting of AT8-IR structures were made using × 25 and × 40 objective lens. The density of IR structures was expressed as the number of structures per mm^2 [33]. Correlations between the density of the IR structures in different areas with the GDS were determined by Spearman's *r* coefficient. Comparisons between the demented and non-demented groups were made using the non-parametric test of Mann-Whitney.

Confocal microscopy

Selected samples were double labeled with the mAb AT8 and the dye thiazin red (TR; Fluka, Busch); after mAb AT8 incubation for 1 h, sections were incubated with fluorescein isothiocyanate (FITC)-tagged goat anti-mouse IgG for 1 h, and washed with PBS-0.2% Triton X-100. Sections were counterstained with TR (0.01% in water) for 5 min, then washed and mounted in an anti-quenching media (Vectashield, Vector Labs). TR is a red fluorescence dye which differentiates between non-fibrillar and fibrillar state of aggregation of tau antigens associated with the PHFs [30]. Double-immunolabeled sections were viewed with a × 60 (N. A. 1.4) oil immersion objective on an epi-fluorescence Nikon microscope with attached confocal system (Bio-Rad MRC 600, Watford, UK). From each area, 10–15 optical Z-sections (around 0.2–0.5 μm thick) were scanned using the dual channel imaging system of the laser confocal microscope. When both channels were merged, the correspondent pseudocolors green for FITC, red for TR and yellow for colocalization were displayed at the monitor screen.

Results

Distribution of AT8-IR structures in demented and non-demented cases

In all the centenarian cases mAb AT8 identified intracellular tangles (I-NFTs), granular diffuse deposits (GDD) in the cytoplasm, as well as neuritic clusters (NCs) and neuritic plaques (NPs) (see Fig. 3 A–H). For morphometry, NPs and NCs were considered together. Neuropil threads were also immunolabeled with mAb AT8, but were not considered in the morphometrical analysis.

When all the cases were analyzed together, layer II of the entorhinal cortex, the subiculum and CA1 areas showed the highest number of AT8-IR structures (Fig. 1). In each region, the number of I-NFTs was significantly higher than any other AT8-IR structure ($P < 0.05$), with the exception of the superior temporal isocortex (Fig. 1).

Correlations between the densities of AT8-IR structures and the GDS

When all the areas were considered together, the density of AT8-IR I-NFTs correlated significantly with the GDS ($r = 0.547$, $P = 0.016$; Table 1), while no significant correlation of the GDS was found with the other two AT8-IR structures (GDD and NC).

Additionally, when each area was analyzed separately, a significant correlation between the densities of AT8-IR I-NFTs and the GDS was found in layer II of the entorhinal cortex ($r = 0.66$, $P = 0.005$) and the subiculum ($r = 0.491$, $P = 0.034$), but not in CA1, regardless of the high number of AT8-IR structures present in this area (Table 1). The density of AT8-IR NCs correlated with GDS in

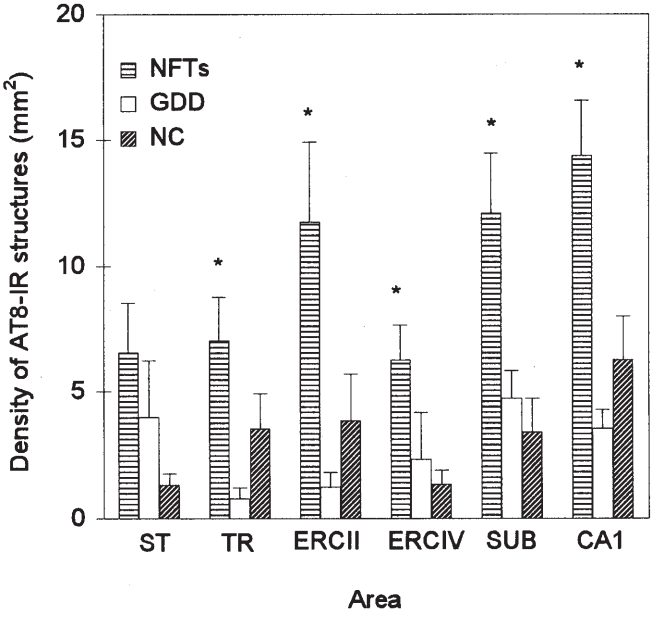

Fig. 1 Regional distribution of AT8-IR structures in a group of demented and non-demented centenarians. Six brain regions were assessed: superior temporal isocortex (*ST*), transentorhinal (*TR*), layer II of the entorhinal cortex (*ERC II*), layer IV of the entorhinal cortex (*ERC IV*), subiculum (*SUB*), and CA1. Three different lesions were quantified: I-NFTs, GDD, NC. Density of lesions corresponds to the average of 19 cases. Lesions are found most frequently in CA1, ERC II and SUB. For each region the statistical significance of differences between the three lesions are indicated with *asterisks* (Student-Newman-Keuls: *$P < 0.05$) (*IR* immunoreactive, *I-NFTs* intracellular tangles, *GDD* intracellular granular diffuse deposits, *NC* neuritic clusters)

layer II of the entorhinal cortex ($r = 0.611$, $P = 0.01$), but not in the other regions (Table 1).

Correlation between the density of AT8-IR structures and the GDS among demented and non-demented centenarians

To distinguish the effects of aging and AD we separated the centenarians into demented and non-demented groups. None of the previous correlations between the densities of these structures and the GDS were obtained when the demented and non-demented centenarian cases were separated (data not shown).

Density of AT8-IR structures in the demented and non-demented groups

Considering all the areas together, the densities of AT8-IR I-NFTs and NCs were significantly higher in the demented group than in the non-demented one ($P < 0.006$ for I-NFTs and $P < 0.001$ for NCs) (Table 2, Fig. 2). When the different areas were analyzed separately, the number of AT8-IR I-NFTs was significantly higher in the demented than in the non-demented group in the transentorhinal ($P = 0.043$), the layer II of the entorhinal cortex ($P = 0.02$), the subiculum ($P < 0.001$) and CA1 ($P = 0.011$). In addition, the number of AT8-IR NCs was significantly higher in the demented group than in non-demented individuals in the transentorhinal region ($P = 0.011$) and layer II of the entorhinal cortex ($P = 0.007$). In constrast, the density of cells with AT8-IR GDD was not significantly different between the two groups (Table 2).

Double labeling with AT8 and TR

For some cases, sections immunolabeled with mAb AT8 were counterstained with the red fluorescent dye, TR, to monitor the state of assembly of abnormally phosphorylated tau protein in both I-NFTs and NCs, using confocal microscopy.

AT8-IR structures of various types were observed mainly in the CA1 area of the hippocampus. These AT8-IR structures displayed differential labeling with TR. The AT8-IR GDD appeared to be an earlier stage of neurofibrillary pathology since they were not detected by TR when they were present in neurons devoid of NFTs (Fig. 3 A). Similar results were obtained by confocal microscopy after immunolabeling with the mAb 423 [30, 31], which recognizes a C-terminal truncation at Glu-391 of the tau protein [35]. As shown in Fig. 3 A, the AT8-IR GDD were distributed throughout the soma and the proximal dendrites. The green immunolabeling was also present in the perikarya. Optical sections through the nuclear area demonstrated that the immunolabeling was associated

Table 1 Correlations between the density of AT8-IR structures and the mental deterioration scale (GDS) (*IR* immunoreactive, *ST* superior temporal isocortex, *TR* transentorhinal, *ERC II/IV* layer II/IV of the entorhinal cortex, *SUB* subiculum, *I-NFT* intracellular neurofibrillary tangles, *GDD* intracellular granular diffuse deposits, *NC* neuritic clusters

Structure	ST	TR	ERC II	ERC IV	SUB	CA1	All areas
I-NFTs	0.264	0.392	*0.660	0.404	*0.491	0.347	*0.547
	0.299	0.107	0.005	0.106	0.034	0.143	0.016
GDD	0.321	–0.121	0.012	–0.242	–0.159	–0.402	–0.304
	0.205	0.627	0.959	0.342	0.508	0.088	0.203
NC	0.334	0.405	*0.611	0.468	0.270	0.296	0.430
	0.188	0.094	0.010	0.059	0.259	0.214	0.066

For each pairwise comparison the correlation coefficient *r* (*upper*) and the significance value *P* (*below*) are given.
* Significant correlation values

Table 2 Comparison of the density of AT8-IR structures between demented and non-demented cases. Analysis by area (*ns* not significant)

Structure	ST	TR	ERC II	ERC IV	SUB	CA1	All areas
I-NFTs	ns	0.043	0.02	ns	< 0.01	0.011	0.006
GDD	ns	ns	ns	ns	ns	ns	ns
NC	ns	0.011	0.007	ns	ns	ns	< 0.001

P values obtained by non-parametric statistics

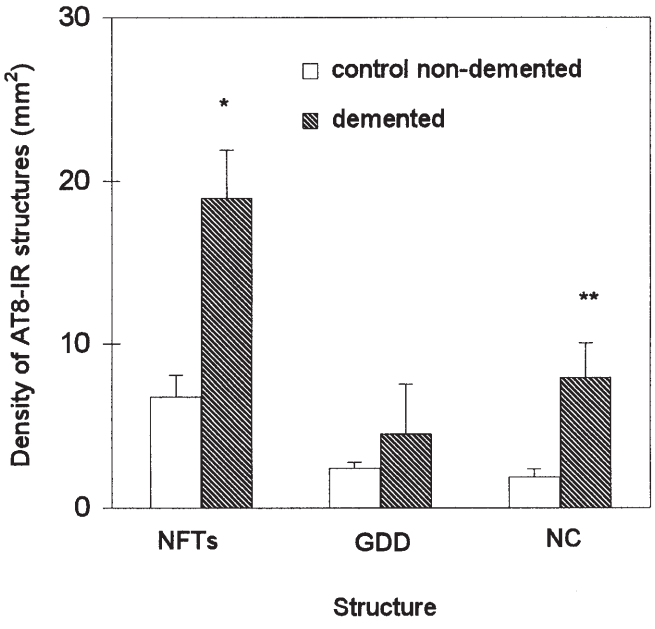

Fig. 2 Density of AT8-IR structures in demented and non-demented cases. The densities of I-NFTs and NC are significantly higher in the demented group than in the non-demented cases (*P = 0.006, **P < 0.001). See the legend for Fig. 1 for the codes

with the nuclear envelope and absent inside the karioplasm (not shown). GDD were not labeled with TR. The earliest evidence of phosphorylated tau aggregation was observed in both the somata and the proximal dendrites (Fig. 3B, C). These structures took the form of doubly labeled "pre-mature tangles" in the somatic compartment varying in number from a single (Fig. 3B) to several deposits (Fig. 3C). These AT8-IR fibrillar aggregates were characteristically associated with the GDD when present in the same cell (arrowhead, Fig. 3B). In a number of AT8-IR cells, aggregates were observed in the soma that were AT8-IR, while "tufts" were observed in the proximal neuritic tree. That the majority of "tufts" were double immunolabeled by mAb AT8 and TR (arrows, Fig. 3D) suggested a state of assembly similar to that observed in the soma. The adjacent neuritic processes remained undetected by TR (arrowhead, Fig. 3D). Typical AT8-IR I-NFTs were characteristically labeled by TR (arrow Fig. 3E). Some tangle-like structures detected by TR in the red channel were not labeled by mAb AT8 (Fig. 4C, D). Autofluorescent lipofuscin deposits were located in the soma and displayed a granular appearance in the red channel (arrowhead, Fig. 3E). AT8-IR I-NFTs mingled with lipofuscin granules were a common finding (Fig. 4A, B).

AT8-IR NCs were found either associated with amyloid-β deposits (Fig. 3F) or as compact clusters without amyloid-β in the vicinity (Fig. 3G). Interestingly, contrasting with the neurites present in the vicinity of the amyloid-β fibrils, which were labeled by the two markers, some compact clusters were labeled by mAb AT8 and differentially by TR, suggesting a differential aggregation state of phosphorylated tau protein in this lesion (arrows, Fig. 3G). A common finding was extracellular tangles labeled by TR (arrows, Fig. 3H) whose associated enlarged neurites were labeled by the mAb AT8 as well as TR (arrowhead, Fig. 3H).

Discussion

There has been considerable controversy regarding the relationship of cognitive dysfunction and neurofibrillary changes occurring in the elderly. In the elderly, the neuropathological changes of amyloid-β plaques and I-NFTs are more confined to the entorhinal cortex and hippocampus rather than spread throughout the neocortex as in AD [5, 8, 36]. However, the usefulness of these findings is limited by the fact that most studies lacked a history of a cognition prior to death [11, 29, 38]. In contrast, those clinicopathological studies that contained the results of prior cognitive testing showed that neuropathological changes in the hippocampus are correlated with cognitive loss [7]. In the present immunocytochemical study, we quantitatively analyzed AT8-IR structures present in the hippocampal formation and the superior temporal isocortex of a group of French centenarians, who have been well documented in previous publications, both for their clinical and neuropathological features [13, 14, 24].

In the present study, we show that layer II of the entorhinal cortex, the subiculum and CA1 contain the highest densities of AT8-IR I-NFTs. The density of I-NFTs was the only parameter that significantly correlated with cognition defined by the GDS (Table 1). I-NFT density in layer II of the entorhinal cortex correlated better with the stage of the mental decline than did I-NFT density in the other regions. In addition, in the same region, the number of AT8-IR NCs also correlated with GDS (Table 1). Taken together, these data support the high vulnerability of layer II entorhinal cortex neurons. Vulnerability of this area to develop NFTs both in the elderly and in AD has been previously reported [10, 22, 23]. In this cohort of centenarians, composed of normal and demented individuals, our results suggest that the extent of neurofibrillary pathology parallels incrementally impairment of cognition.

Most studies have correlated the severity of cognitive impairment in AD with development of NFTs and NPs in the neocortex [1, 3, 16, 27, 34] and not in the entorhinal cortex or hippocampus. The latter regions are less studied for clinicopathological correlation since NFTs are present in normal aging [3, 10, 16, 27]. In the centenarian cases analyzed in this study, the number of AT8-IR NFTs in de-

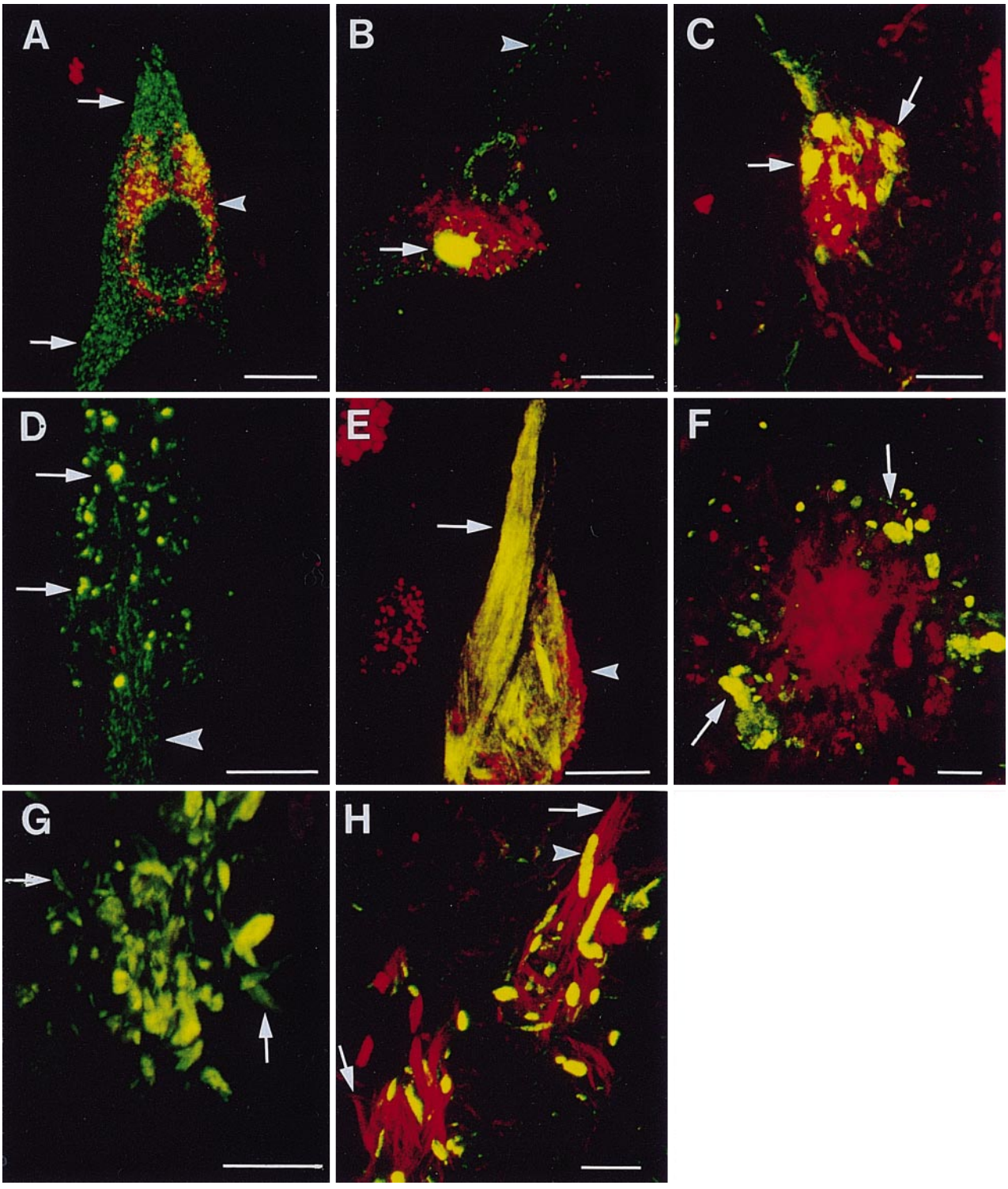

Fig. 3 A–H Double immunolabeling with mAb AT8 and TR. In merged images, colocalization of AT8-IR (*green*) and TR labeling (*red*) is seen as a *yellow* pseudocolour. **A** GDD in the cytoplasm, nuclear membrane and proximal dendrites in a pathological cell (*arrows*). Autofluorescent lipofuscin with a granular appearance is commonly found in the red channel (*arrowhead*). **B** In some cells, besides the presence of GDD (*arrowhead*), "pre-mature tangles" (*arrow*) are also present in the cytoplasm. **C** In the same cell a variety of immunoreactive structures are seen which may correspond to "pre-mature tangles" and distributed toward the nucleus (*arrows*). **D** In some cells, "tufts" in the proximal neuritic tree were double labeled by mAb AT8 and TR (*arrows*). An adjacent neuritic process is also detected in the green channel (*arrowhead*). **E** Double labeling with mAb AT8 and TR of an intracellular tangle (*arrow*). Autofluorescent granules are detected only in the red channel (*arrowhead*). **F** Typically, the neuritic clusters associated with β-amyloid deposits are double labeled with mAb AT8 and TR (*arrows*). **G** Some neurites of the compact clusters not associated with amyloid-β deposits, were labeled by mAb AT8 but not by TR (*arrows*). **H** Extracellular NFTs (*arrows*) lose mAb AT8 immunoreactivity (*green*) but preserve binding sites to TR (*red*). The neurites present in the vicinity are double labeled by the two markers (*arrowhead*) (TR thiazin red). Bars **A**–**H** = 10 μm

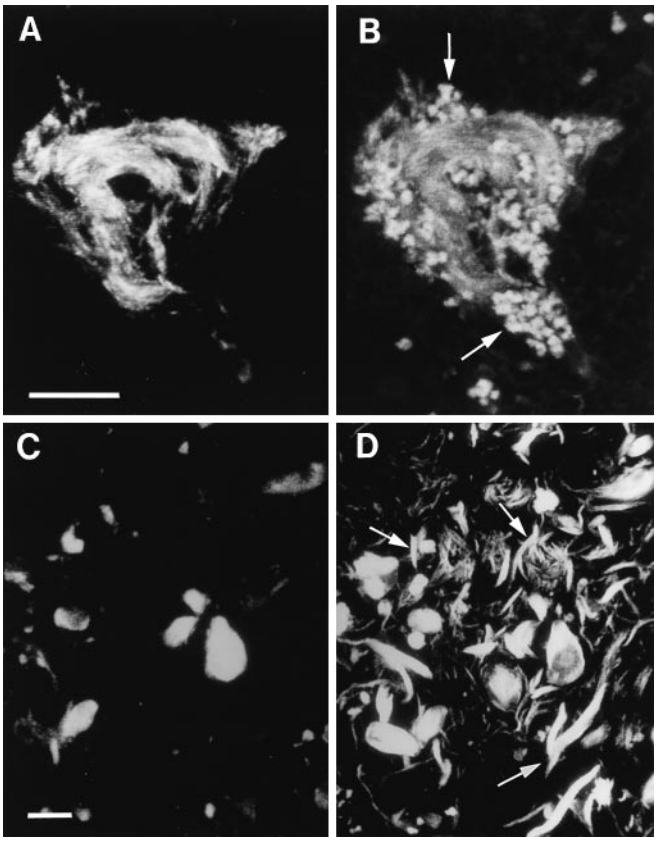

Fig. 4 A–D Double immunolabeling with mAb AT8 and TR. **A**, **B** mAb AT8-IR NFT detected in the green channel (**A**) is mingled with autofluorescent of lipofuscin deposits fluorescing in the red channel (*arrows* in **B**). **C, D** Some NFTs and dystrophic elements which are detected by TR (*arrows in **D***) are not immunolabeled with mAb AT8 (**C**). Bars = 10 μm

mented cases was significantly higher in the subiculum, layer II of the entorhinal cortex, transentorhinal cortex and CA1, when compared with the same regions in non-demented cases (Table 2). Similar differences were found for the density of NCs in layer II of the entorhinal cortex and transentorhinal area. No neuropathological difference between both groups was found in the superior temporal isocortex. These findings support the view that even with substantial cortical involvement, the key to dementia is involvement of the perforant pathway.

I-NFT formation appears to be preceded by accumulation of abnormally phosphorylated tau protein in a non-assembled state [2, 7], suggesting that this process is one of the earliest cytoskeleton abnormalities. Similar IR patterns have been observed in normal non-demented cases using mAb 423 [31], which identifies a truncation at the Glu-931 of the PHF-associated tau protein [35].

TR labeling demonstrated differential states of aggregation of abnormally phosphorylated tau protein in neurons. In particular, the "pre-mature" tangles (Fig. 3 B, C) appear to originate in more than one site in the soma. In later stages, the smaller tangles appear to have fused and form the typical I-NFT (Fig. 3 E). "Pre-mature" tangles may correspond to the group 2 of Braak in which the same mAb AT8 was employed [7]. The observation of AT8-IR NFTs mingled with the granular deposits of lipofuscin suggests that lipofuscin may contribute to NFT formation (Fig. 4 A, B). AT8-IR was also seen in a perinuclear location in some cells lacking binding sites to TR, suggesting a non-fibrillar state. A previous study has described the presence of tau immunoreactivity inside the nucleus rather than on the outer membrane [9]. It certainly suggests that perinuclear tau accumulation can act as an organizing "center" for the assembly of "pre-mature tangles" that subsequently progress to I-NFTs.

Double labeling with mAb AT8 and TR for extraneuronal NFTs (Fig. 3 H) shows they have lost all AT8-IR, as a result of extracellular proteolysis, while they are still detected by TR (a dye with high affinity for β-pleated-sheet-assembled structures). Similar results were found in a population of dystrophic neurites, also suggesting their extracellular nature (Fig. 4 C, D).

In general, these findings using double labeling confocal microscopy indicate that abnormally phosphorylated tau protein is present in different stages of assembly in both tangles and neurites.

In summary, our study of centenarians shows that the density of neurofibrillary structures in the hippocampus of demented cases was significantly higher than in the non-demented individuals. Strikingly, neurons from the perforant pathway showed the greatest increase in demented versus non-demented cases. These findings support the view that the dementia of AD marks a clear departure from normal aging even in the oldest old. In addition, our results show that tau deposits in a non-fibrillar state did not correlate significantly with dementia status as tangles do.

Acknowledgements We wish to thank Dr. George Perry for critical reading and editorial comments. This work was supported by a grant from CONACyT-26319M (México) to R. M. For this project F. G.-S. received financial support from CONACyT (México)

References

1. Arriagada PV, Growdon JH, Hedley-Whyte ET, Hyman BT (1992) Neurofibrillary tangles but not senile plaques parallel duration and severity of Alzheimer's disease. Neurology 42: 631–639
2. Bancher C, Brunner C, Lassmann H, Budka H, Jellinger K, Wiche G, Seitelberger F, Grundke-Iqbal Y, Iqbal K, Wisniewski HM (1988) Accumulation of abnormally phosphorylated τ precedes the formation of neurofibrillary tangles in Alzheimer's disease. Brain Res 477: 90–99
3. Bierer LM, Hof PR, Purohit DP, Carlin L, Schmeidler J, Davies KL, Perl DP (1995) Neocortical neurofibrillary tangles correlate with dementia severity in Alzeimer's disease. Arch Neurol 52: 81–88
4. Biernat JM, Mandelkow EM, Schröter C, Lichtenberg-Kraag B, Steiner B, Berling B, Meyer H, Mercken M, Vandermeeren A, Goedert M, Mandelkow E (1992) The switch of tau protein to an Alzheimer-like state includes the phosphorylation of two serine-proline motifs upstream of the microtubule binding region. EMBO J 11: 1593–1597

5. Bouras C, Hof PR, Morrison HJ (1993) Neurofibrillary tangle densities in the hippocampal formation in a non-demented population define subgroups of patients with differential early pathologic changes. Neurosci Lett 153:131–135
6. Bouras C, Hof PR, Giannakopoulos P, Michel JP, Morrison JH (1994) Regional distribution of neurofibrillary tangles and senile plaques in the cerebral cortex of elderly patients: A quantitative evaluation of one-year autopsy population from a geriatric hospital. Cereb Cortex 4:138–150
7. Braak E, Braak H, Mandelkow EM (1994) A sequence of cytoskeleton changes related to the formation of neurofibrillary tangles and neuropil threads. Acta Neuropathol 87:554–567
8. Braak H, Braak E (1991) Neuropathological stageing of Alzheimer-related changes. Acta Neuropathol 82:239–259
9. Brady RM, Zinkowski RP, Binder LI (1995) Presence of tau in isolated nuclei from human brain. Neurobiol Aging 16:479–486
10. Cras P, Smith MA, Richey PL, Siedlak SL, Mulvihill P, Perry G (1995) Extracellular neurofibrillary tangles reflect neuronal loss and provide further evidence of extensive protein cross-linking in Alzheimer's disease. Acta Neuropathol 89:291–295
11. Crystal HA, Dickson DW, Sliwinksi MJ, Lipton RB, Grober E, Marks-Nelson H, Antis P (1993) Pathological markers associated with normal aging and dementia in the elderly. Ann Neurol 34:566–573
12. Delacourte A, Flament S, Dibe EM, Hublau P, Sablonniere B, Hemon B, Scherrer V, DeFossez A (1990) Pathological proteins Tau 64 and 69 are specifically expressed in the somatodendritic domain of the degenerating cortical neurons during Alzheimer's disease. Acta Neuropathol 80:111–117
13. Delaère P, He Y, Fayet G, Duyckaerts C, Hauw JJ (1993) βA4 deposits are constant in the brain of the oldest old: an immunocytochemical study of 20 French centenarians. Neurobiol Aging 14:191–194
14. Fayet G, Hauw JJ, Delaère P, He Y, Duyckaerts C, Beck H, Forette F, Gallinari C, Laurent M, Moulias R, Piette F, Sachet A (1994) Neuropathology of 20 centenarians. I. Clinical data. Rev Neurol (Paris) 150:16–21
15. Flament S, DeLacourte A, Hemon B, DeFossez A (1989) Characterization of two pathological tau protein variants in Alzheimer brain cortices. J Neurol Sci 92:133–141
16. Geddes JW, Snowdon DA, Soultanian NS, Tekirian KP, Riley JW, Davis DG, Markesbery WR (1996) Braak stages III–IV of Alzheimer-related neuropathology are associated with mild memory loss, stages V–VI are associated with dementia: findings from the Nun Study. J Neuropathol Exp Neurol 55:617
17. Giannakopoulos P, Hof PR, Mottier S, Michel JP, Bouras C (1994) Neuropathological changes in the cerebral cortex of 1258 cases from a geriatric hospital: retrospective clinicopathological evaluation of a 10-year autopsy population. Acta Neuropathol 87:456–468
18. Giannakopoulos P, Hof PR, Vallet PG, Giannakopoulos AS, Charnay Y, Bouras C (1995) Quantitative analysis of neuropathologic changes in the cerebral cortex of centenarians. Prog Neuropsychopharmacol Biol Psychiatry 19:577–592
19. Giannakopoulos P, Hof PR, Giannakopoulos AS, Herrmann FR, Michel JP, Bouras C (1995) Regional distribution of neurofibrillary tangles and senile plaques in the cerebral cortex of very old patients. Arch Neurol 52:1150–1159
20. Goedert M, Jakes R, Crowther RA, Six J, Lübke U, Vandermeeren M, Cras P, Trojanowski JQ, Lee VM-Y (1993) The abnormal phosphorylation of tau protein at Ser-202 in Alzheimer's disease recapitulates phosphorylation during development. Proc Natl Acad Sci USA 90:5066–5070
21. Goedert M, Jakes R, Vanmechelen E (1995) Monoclonal antibody AT8 recognises tau protein phosphorylated at both serine 202 and threonine 205. Neurosci Lett 189:167–169
22. Gómez-Isla T, Price JL, McKeel DW, Morris JC, Growdon JH, Hyman BT (1996) Profound loss of layer II entorhinal cortex neurons occurs in very mild Alzheimer's disease. J Neurosci 16:4491–4500
23. Gómez-Isla T, Hollister R, West H, Mui S, Growdon JH, Petersen RC, Parisi JE, Hyman BT (1997) Neuronal loss correlates with but exceeds neurofibrillary tangles in Alzheimer's disease. Ann Neurol 41:17–24
24. Hauw JJ, Vignolo P, Duyckaerts C, Beck H, Forette F, Henry JF, Laurent M, Piette F, Sachet A, Berthaux P (1986) Neuropathological study of 12 centenarians: the incidence of Alzheimer type senile dementia is not particularly increased in this group of very old patients. Rev Neurol (Paris) 142:107–115
25. Itoh Y, Yamada M, Suematsu N, Matsushita M, Otomo E (1998) An immunohistochemical study of centenarian brains: a comparison. J Neurol Sci 157:73–81
26. Katzman R, Terry R, DeTeresa R, Brown T, Davies P, Fuld P, Renbing X, Peck A (1988) Clinical, pathological, and neurochemical changes in dementia: a subgroup with preserved mental status and numerous neocortical plaques. Ann Neurol 23:138–144
27. Kazze AM, Eskin TA, Lapham LW, Gabriel KR, McDaniel KD, Hamill RW (1993) Clinicopathologic correlates in Alzheimer's disease: assessment of clinical and pathologic diagnostic criteria. Alzheimer Dis Assoc Disord 7:152–164
28. Lee VMY, Balin BJ, Otvos L, Trojanowski JQ (1991) A68: a major subunit of paired helical filaments and derivatized forms of normal tau. Science 251:675–678
29. Mann DMA, Tucker CM, Yates PO (1987) The topographic distribution of senile plaques and neurofibrillary tangles in the brains of non-demented persons of different ages. Neuropathol Appl Neurobiol 13:123–139
30. Mena R, Edwards P, Pérez-Olvera O, Wischik CM (1995) Monitoring pathological assembly of tau and β-amyloid proteins in Alzheimer's disease. Acta Neuropathol 89:50–56
31. Mena R, Edwards P, Harrington CR, Mukaetova-Ladinska EB, Wischik CM (1996) Staging the pathological assembly of tau protein into paired helical filaments in Alzheimer's disease. Acta Neuropathol 91:633–641
32. Morris JC, Storandt M, McKeel DW, Rubin EH, Price JL, Grant EA, Berg L (1996) Cerebral amyloid deposition and diffuse plaques in "normal" aging: evidence for presymptomatic and very mild Alzheimer's disease. Neurology 46:707–719
33. Mukaetova-Ladinska EB, Harrington CR, Roth M, Wischik CM (1993) Biochemical and anatomical redistribution of tau protein in Alzheimer's disease. Am J Pathol 143:565–578
34. Nagy ZS, Esiri MM, Jobst KA, Morris JH, King EMF, McDonald B, Litchfield S, Smith A, Barnetson L, Smith AD (1995) Relative roles of plaques and tangles in the dementia of Alzheimer's disease: correlations using three sets of neuropathological criteria. Dementia 6:21–31
35. Novak M, Kabat J, Wischik CM (1993) Molecular characterization of the minimal protease resistant tau unit of the Alzheimer's disease paired helical filaments. EMBO J 12:365–370
36. Pearson RCA, Esiri MM, Hiorns RW, Wilcock GK, Powell TPS (1985) Anatomical correlates of the distribution of the pathological changes in the neocortex in AD. Proc Natl Acad Sci USA 82:4531–4534
37. Schmitt FA, Wekstein DR, Davies D, Beuscher A, Markesbery WR (1994) Neuropathological findings in cognitively normal older adults. Neurobiol Aging 15:S109–S110
38. Tomilson BE, Blessed G, Roth M (1968) Observations on the brains of non-demented old people. J Neurol Sci 7:331–356
39. Vermersch P, David JP, Frigard B, Fallet-Bianco C, Wattez A, Petit H, Delacourte A (1995b) Cortical mapping of Alzheimer pathology in brains of aged non-demented subjects. Prog Neuropsychopharmacol Biol Psychiatry 19:1035–1047